Direct lattice imageing in single crystals of isotatic polystyrene

Masaki Tsuji, Saroj K. Roy and R. St. John Manley
Pulp and Paper Research Institute of Canada and Department of Chemistry, McGill University, Montreal, Quebec, Canada, H3A 2A7
(Received 20 January 1984)

Lattice lines with 1.1 nm and 0.55 nm spacings were resolved in isotactic polystyrene (i-PS) single crystals using a conventional transmission electron microscope, equipped for low dose imageing. It is suggested that these crystals may be used as a model for the direct imageing of structural defects in polymer crystals.

(Keywords: low-dose imageing; isotactic polystyrene; beam sensitive material; radiation damage; lattice resolution; electron microscopy)

INTRODUCTION

Modern electron microscopes are capable of such high resolution that direct observation of crystal structure is possible on a molecular or atomic level[1]. It is, however, difficult in practice to study electron-beam sensitive materials at such a level. Most polymer crystals are susceptible to electron irradiation damage and are brought to an amorphous state by a relatively small irradiation dose. Thus lattice imageing of polymer crystals is not easy and it has been achieved for only a few polymers, notably poly(*p*-xylylene)[2,3], poly(*p*-phenylene terephthalamide)[4], poly[1,6,di(*N*-carbazolyl)-2,4-hexadiene][5] and poly(*p*-phenylene benzobis-thiazole)[6]. Recently one-dimensional lattice imageing of Valonia cellulose was reported[7], but it was achieved by using a special cryo-stage (4.2°K) combined with a superconducting lens system[7]. In this paper we report axial bright field lattice imageing of isotactic polystyrene (i-PS) single crystals using a conventional transmission electron microscope (EM).

EXPERIMENTAL

Sample preparation

The sample used was i-PS (Dow Chemical Company) with a viscosity-average molecular weight, M_v of 2.08×10^6. Atactic material was removed by refluxing the polymer several times in 2-butanone, followed by hot-filtration and vacuum drying. The crystallization procedure was essentially the same as used by Keith *et al.*[8]. The polymer was dissolved in 2:1 (v/v) n-tetradecane/decalin (mixture of *cis*- and *trans*-isomers) under a nitrogen atmosphere. The solution (0.3 wt%) was cooled to 180°C, held at this temperature for 2–3 days and then cooled to the room temperature.

Electron microscopy

The detailed procedure for electron microscopy will be described elsewhere[9]; here only an outline is given. The specimen was mounted on electron microscope grids coated with a thin carbon supporting film and examined without shadowing with a Philips EM400T electron microscope (hair-pin filament) which was operated at 120 kV with a liquid nitrogen anti-contamination trap. The spherical abberation coefficient was measured as 3.0 ± 0.4 mm at 120 kV using Johansen's method[10]. The size of the objective aperature was 50 μm which allowed all diffracted beams up to the 33.0 reflections to be used for high resolution imageing.

The beam intensity (i.e. brightness) was carefully chosen to produce an average optical density of about 0.5*D* on the micrograph and to suppress damping of the phase contrast transfer function due to the illuminating angle[11]. Under the conditions used the attainable resolution was 0.5 nm. The EM images were recorded on Kodak EM film 4489 using the Philips Low Dose Unit PW 6587[12] to minimize radiation damage. The mechanism of operation of this device is essentially the same as proposed by Fujiyoshi *et al.*[13]. The exposed EM films were developed at 20°C for 4 min with Kodak developer D-19 diluted 1:2 and fixed with Kodak rapid fixer. The micrographs were analysed by using a Polaron electron micrograph optical diffractometer.

To record electron diffraction patterns, Kodak Tri-X Ortho Film 4163 was used. The films were developed at 20°C for 7 min with D-19 (full strength) containing a small amount of Kodak anti-fog No. 1 (AF-70). The electron beam current (i.e. the screen current) was measured by converting the reading of the exposure meter installed in the microscope to total screen current using a chart supplied by Philips.

RESULTS AND DISCUSSION

Figure 1 shows the typical appearance of the solution-grown crystals of i-PS: two types could be distinguished, namely hexagonal single crystals with spiral overgrowth (A) and irregular-shaped aggregates of crystalline platelets (B). Both types gave the characteristic electron diffraction pattern of the i-PS crystal lattice with hexagonal symmetry. The lamellar thickness

0032-3861/84/111573-04$03.00

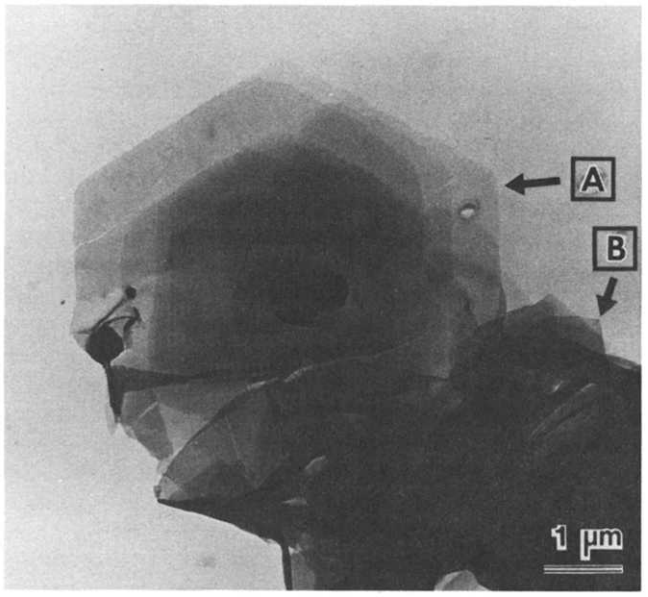

Figure 1 Single crystals of i-PS grown at 180°C from 0.3 wt% solution in a mixed solvent of 2:1 (v/v) n-tetradecane/decalin (100 kV, without shadowing). (a) A typical hexagonal crystal with spiral overgrowth. (b) A portion of an irregular shaped aggregate of crystalline platelets

measured with the shadowing technique was approximately 100 Å.

Figure 2 shows the change of the selected-area electron diffraction pattern of an i-PS single crystal with increasing electron irradiation dose. The pattern was indexed as proposed by Blais and Manley[14] on the basis of a trigonal unit cell whose lattice dimensions are: $a=b=2.19$ nm, c(chain axis)$=0.665$ nm[15,16]. As illustrated in *Figure 2(a)* the pattern is characterized by very strong 22.0 and strong 11.0 and 30.0 reflections, corresponding to lattice spacings of 1.1 nm, 0.55 nm and 0.63 nm, respectively. Reflections enclosed by circles are very faint, but can be recognized on the original negative. *Figure 2* shows that the crystalline reflections disappear sequentially, starting from the higher orders, with increasing irradiation dose and the 11.0 reflections are the most stable. The 11.0 reflections still exist in *Figure 2(e)* which was recorded at a dose of 0.0165 Coulomb cm^{-2} and disappeared completely in *Figure 2(f)* recorded at 0.0202 Coulomb cm^{-2}. Thus the total end point dose, TEPD, (i.e. the electron irradiation dose necessary for complete disappearance of all crystalline reflections in the diffraction pattern) of i-PS single crystals was measured as about 0.02 Coulomb cm^{-2} at 120 KV and room temperature. This value is about 5–6

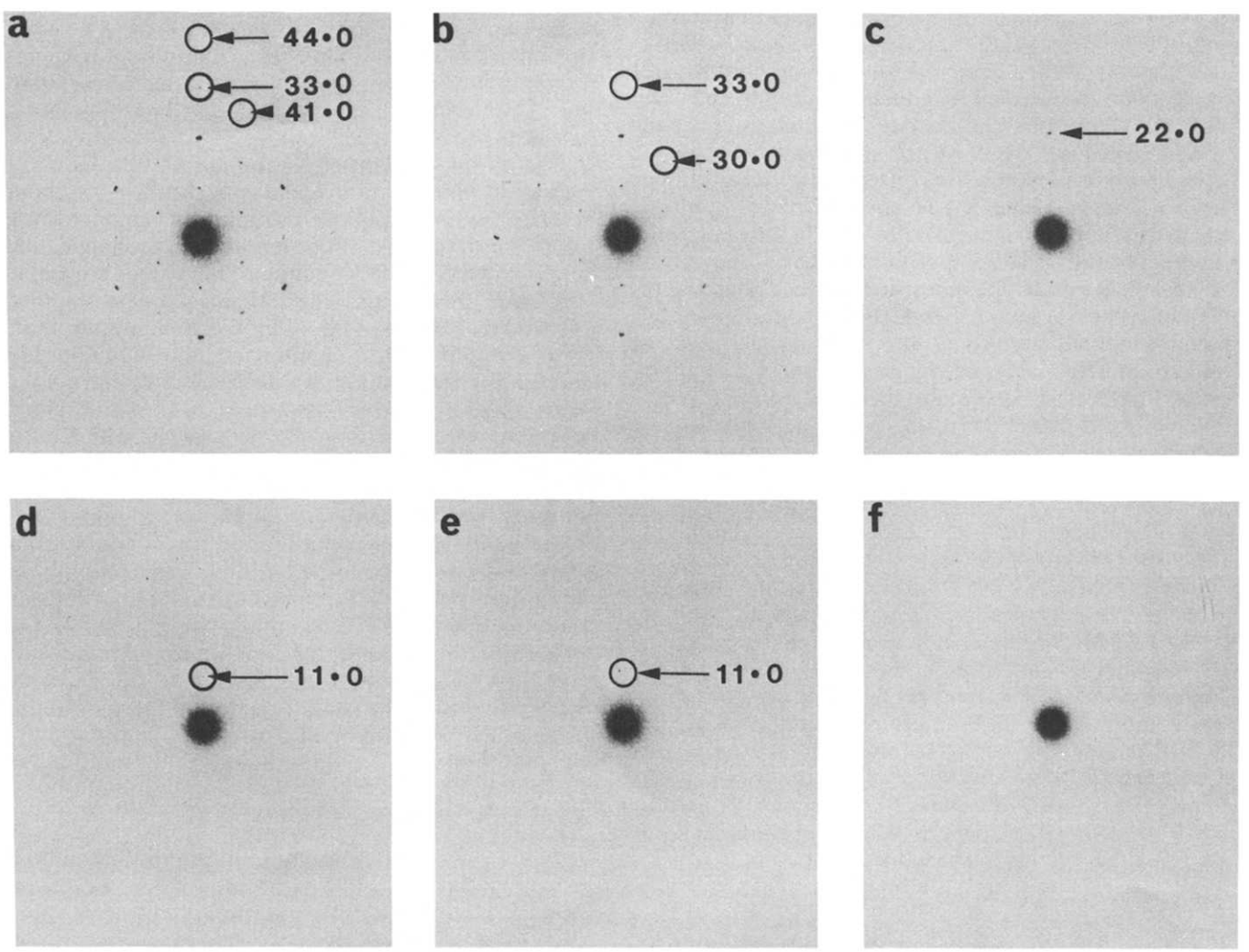

Figure 2 The selected-area electron diffraction pattern of an i-PS single crystal at an irradiation dose of (a) 0.1×10^{-3}, (b) 4.2×10^{-3}, (c) 8.3×10^{-3}, (d) 12.4×10^{-3}, (e) 16.5×10^{-3}, (f) 20.2×10^{-3} Coulomb cm^{-2}. Reflections enclosed by circles are very faint, but can be easily recognized on the original negatives

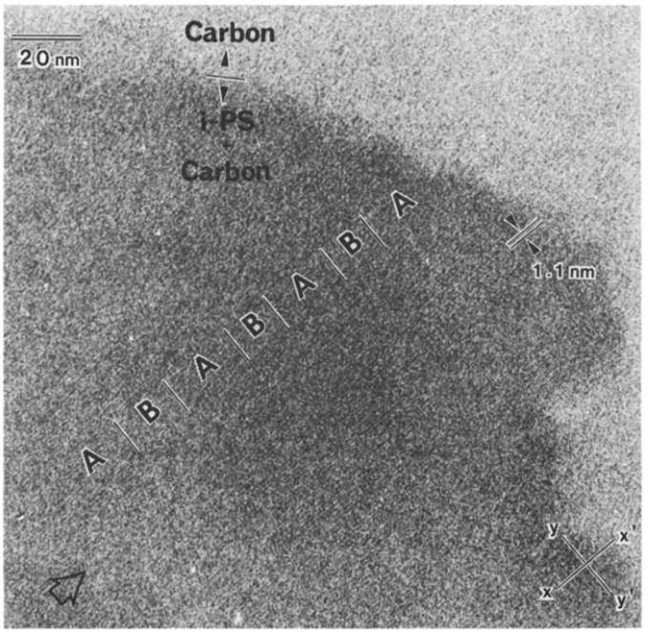

Figure 3 Axial bright field lattice image of the edge of an i-PS single crystal. 1.1 nm lattice fringes can be seen by inspection in the direction indicated by the arrow

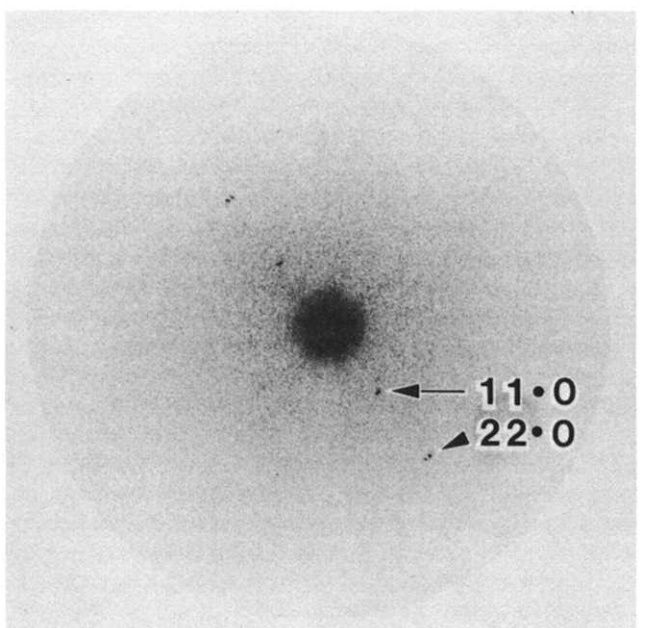

Figure 4 Optical diffractogram of *Figure 3*. The orientation of this Figure corresponds to that of *Figure 2*. Reflections corresponding to (11.0) and (22.0) lattice planes can be seen

times greater than that of polyethylene crystals. Taking into consideration the TEPD of i-PS, the granularity and characteristic curve of the EM film (Kodak 4489) for 120 kV electrons, an instrumental magnification of 36000 was adopted. Details of the criteria that were used to determine the optimum magnification will be given elsewhere[9]. It should be noticed, however, that the magnitude of the TEPD of i-PS corresponds to the dose necessary to obtain only one negative at this magnification. Therefore lattice imageing of i-PS crystals would be almost impossible without the Low Dose Unit.

Figure 3 shows the resulting high resolution electron micrograph of the edge of an i-PS single crystal. Close observation in the direction X–X′ reveals one-dimensional lattice fringes with a spacing of 1.1 nm, corresponding to the (11.0) lattice planes. The optical diffraction pattern of the micrograph (see *Figure 4*) shows 22.0 and 11.0 reflections corresponding to lattice spacings of 0.55 and 1.1 nm respectively. However, lattice fringes corresponding to the 22.0 reflection cannot be recognized in the image (*Figure 3*), probably because of the low signal-to-noise ratio due to the photographic graininess.

Further inspection of *Figure 3* reveals an apparent band structure in which two alternating zones, A and B, can be recognized. Lattice fringes can be observed in the A bands but not in the B bands. Two possible explanations of this phenomenon can be envisaged. The first relates to irradiation damage, while the second is based upon misorientation of the (11.0) lattice planes. Taking into account the periodical nature of the band structure (the width of the bands is 15–20 nm) the latter explanation seems more reasonable. It is therefore proposed that in the B bands the Bragg condition for 11.0 reflections may not be satisfied. *Figure 5* shows the rocking curve calculated kinematically for the (11.0) reflection, where a crystal thickness of 10 nm was assumed and the Ewald sphere was regarded as an approximately flat plane[17,18]. A deviation of about 6° is sufficient for almost complete extinction of the 11.0 reflection. Accordingly it can be deduced that the single crystal observed here is not perfectly flat but somewhat undulating. The 22.0 and 11.0 reflections in *Figure 4* are split into two spots. This seems to suggest that there is a difference of orientation between bands. More detailed

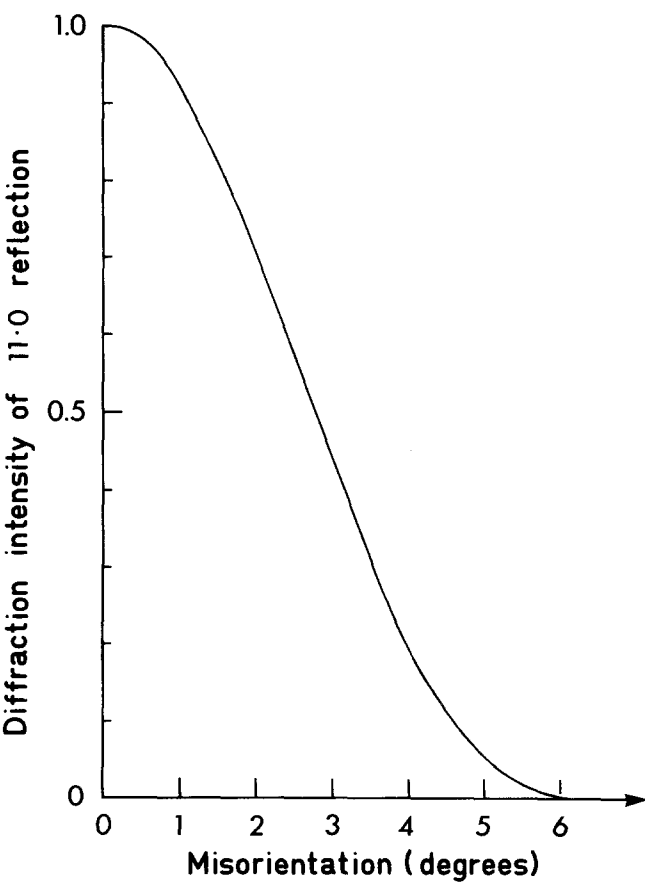

Figure 5 Calculated rocking curve for a 10 nm thick single crystal of i-PS with (11.0) planes in the Bragg position

discussion of the nature and origin of this phenomenon must, however, await further study.

In summary, the present work has demonstrated that direct lattice images of i-PS single crystals can be obtained in a conventional transmission electron microscope using low dose imageing. This suggests that i-PS single crystals may serve as a model for the direct imageing of structural defects in polymer crystals and the study of such defects in relation to properties known to be affected by them.

REFERENCES

1 For example, Proc. 47th Nobel Symposium, Lidingö, 1979 'Direct Imaging of Atoms in Crystals and Molecules', (Ed. L. Kihlborg), Royal Swedish Academy of Sciences, Stockholm; Chemica Scripta, **14**, (1978–79)
2 Bassett, G. A. and Keller, A. *Koll-Z.* 1969, **231**, 386
3 Tsuji, M., Isoda, S., Ohara, M., Kawaguchi, A. and Katayama, K. *Polymer* 1982, **23**, 1568
4 Dobb, M. G., Hindeleh, A. M., Johnson, D. J. and Saville, B. P. *Nature* 1975, **253**, 189
5 Read, R. T. and Young, R. J. *J. Mater. Sci.* 1981, **16**, 2922
6 Shimamura, K., Minter, J. R. and Thomas, E. L. *J. Mater. Sci. Lett.* 1983, **2**, 54
7 Knapek, E. *Ultramicroscopy* 1982, **10**, 71
8 Keith, H. D., Vadimsky, R. G. and Padden, Jr., F. J. *J. Polym. Sci., A-2* 1970, **8**, 1687
9 Tsuji, M., Roy, S. K. and St. J. Manley, R. To be published
10 Johansen, B. V. *Micron* 1973, **4**, 446
11 Tsuji, M. and St. J. Manley, R. *J. Microscopy* 1983, **130**, 93
12 Handbook of 'Low Dose Unit for EM400', Philips, 1979
13 Fujiyoshi, Y., Kobayashi, T., Ishizuka, K., Uyeda, N., Ishida, Y. and Harada, Y. *Ultramicroscopy* 1980, **5**, 459
14 Blais, P. and St. J. Manley, R. *J. Polym. Sci. A-2* 1966, **4**, 1022
15 Natta, G. and Corradini, P. *Makromol. Chem.* 1955, **16**, 77
16 Natta, G., Corradini, P. and Bassi, I. W. *Nuova Cimento* (Suppl.) 1960, **15**, 68
17 Hirsch, P. B., Howie, A., Nicholson, R. B., Pashley, D. W. and Whelan, M. J. in 'Electron Microscopy of Thin Crystals', Butterworths, London, 1965
18 Cowley, J. M. in 'Diffraction Physics', North-Holland, Amsterdam, p. 183, 1975